Journal of Sustainable Metallurgy (2020) 6:216–226
https://doi.org/10.1007/s40831-020-00262-x

THEMATIC SECTION: SLAG VALORISATION

The Impact of Sample Homogeneity, Crucible Material, and Oxygen Partial Pressure on the Crystallization of Fe-Rich Oxidic Slag in CLSM Experiments

Jan Peter Schupsky[1] · Muxing Guo[2] · Bart Blanpain[2] · Michael Müller[1]

Published online: 31 January 2020

Abstract
Crystallization tendency and the state of oxidic slags are important influencing factors for slag viscosity and therefore slag tapping. During the gasification process slag is constantly produced and flows down the gasifier walls until it is intercepted and stored for further treatment or a possible valorisation. The kinds of fuel used for gasification lead to different kinds of slag composition likewise. Slag viscosity is strongly influenced by the composition of the slag and the temperature. However, the process of crystallization represents another major influencing factor. Slag crystallization is also affected by several parameters, whose effects need to be considered in experimental studies. This study investigated the impact of the sample state, the chosen crucible material, and the oxygen partial pressure on the crystallization of a Fe-rich oxidic slag in the confocal laser scanning microscope (CLSM) experiment. Using sample powder may lead to heterogeneous nucleation and crystallization during heating due to heterogeneous melting of the compounds. The selection of crucible material is crucial to prevent alloy formation of Fe-species with Pt-crucibles under reducing atmosphere. Finally, the partial pressure of oxygen influences the crystallization tendency as well as the morphology of the crystallized phases. These parameters impede the reproducibility of results as well as the comparison with results deriving from other experiments like sample quenching. This contribution provides an enhanced understanding of the stated parameter effects on the experimental investigation of oxidic slags using the CLSM setup and yields advice to prevent experimental influence on the results.

Keywords Crystallization · Gasifier slag · CLSM · Process parameters · Reducing atmosphere · Sample annealing

Introduction

The energy transition is one of the major tasks for mankind in modern days, as the transition from fossil fuels to renewable energies needs tremendous effort. Therefore, the demand for bridging technologies is high and the usage of gasification technology serves advantages compared to combustion plants [1, 2]. Gasifiers, such as entrained flow gasifiers, are able to convert different kinds of fuels (coal, biomass, waste) into energy [3]. Also, the operation under partial load conditions gives gasification technology a high relevance by filling gaps in the power grid due to fluctuations of renewable energy production [4, 5]. During entrained flow gasification, slag is produced constantly under reducing conditions. The slag adheres on the refractory walls, flows down, and prevents slag blocking [1, 6]. However, changes of the slag's state, such as crystallization, influence its viscosity and fluid behavior [7]. Furthermore, gasifier slags are used in the construction industry as a concrete additive to enhance

The contributing editor for this article was Sharif Jahanshahi.

✉ Jan Peter Schupsky
j.schupsky@fz-juelich.de

Muxing Guo
muxing.guo@kuleuven.be

Bart Blanpain
bart.blanpain@kuleuven.be

Michael Müller
mic.mueller@fz-juelich.de

[1] Institute of Energy- and Climate Research – IEK 2, Forschungszentrum Jülich GmbH, 52428 Jülich, Germany

[2] Department of Materials Engineering, KU Leuven, 3001 Leuven, Belgium

mechanical strength. Accordingly, a fully glassy slag with an isotropic structure is preferably used, while crystallization hinders its usage due to its anisotropic structural character.

Slag crystallization investigations have been performed by several authors in the recent years [8–10]. As the crystallization phenomenon is barely understood, experimental investigations on crystallization kinetics and products are favored in science. The single hot thermocouple technique (SHTT) is widespread experiment used by several authors for determining crystallization kinetics [9, 11]. However, those studies often separate the slag crystallization products from the crystallization kinetics as well as from thermodynamic equilibrium calculations [8, 9, 11]. To fully understand the impact of crystallization on the slag viscosity, a fundamental understanding of crystal phase formation in the investigated slags is required. Therefore, a solid and reliable experimental base needs to be provided. However, this study shows that the performance of experiments affords a sensitive handling, since the results can be majorly influenced by certain parameters, as described in the following.

Firstly, this study displays the crystallization products that are predicted under equilibrium conditions by using FactSage Equilib program and GTox database. Secondly, the influence of sample homogeneity, the oxygen partial pressure, and interactions of the sample with the crucible material during experimental operation is examined. Additionally, this study provides helpful advice for experimental investigations of oxidic slags, to reduce sources of error and to improve the reproducibility of results. Investigations were conducted with a confocal laser scanning microscope (CLSM) [3]. The experiments proved that the usage of sample powder entails a heterogeneous crystallization even at high temperatures of above 1500 °C. The crystallized phases changed the composition of the slag bulk, hence crystallization results are not representative. The partial pressure of oxygen also affects the crystallization tendency. Higher oxygen partial pressures lead to higher melting points and to faster crystallization kinetics. Pt is commonly used as the crucible material and interacts with Fe-rich slags under reducing conditions. An alloy is formed that causes the crucible to disintegrate subsequently. The usage of Mo-crucibles instead is more reasonable due to its high melting point and no alloy formation with Fe-containing species.

Methods

Sample Preparation

Based on previous coal ash analysis [12], the Fe-rich synthetic coal ash system HKR was analyzed (Table 1). It was chosen to perform the experiments with synthetic slag samples for several reasons. Firstly, the generation of real gasifier slag is often poorly documented and chemical fluctuations may occur, analogue to the fluctuations of the fuels composition. Secondly, the renounce of alkalis reduces volatility of the slag sample. As a result, no change of the bulk composition occurs and no alkali-containing compounds condensed in the experimental apparatus. The amount of compounds was reduced to SiO_2, Al_2O_3, CaO, MgO, and Fe_2O_3, respectively. Those five oxides represent slightly more than 95% of the overall compounds of the real HKR coal slag [12].

Table 1 Composition of the analyzed synthetic slag system in wt%

	SiO_2	Al_2O_3	CaO	Fe_2O_3	MgO
Synthetic HKR slag	34.8	12.0	27.4	14.5	11.4

The synthetic oxide slag was produced using high-purity oxides (Alfa Aesar, Massachusetts, U.S. and Merck, Darmstadt, Germany). Oxides were balanced, mixed, and subsequently dried at 100 °C to release adhered humidity. The oxide mixture was blended for 24 h with addition of millstones to reduce the grain size, resulting in homogenized synthetic slag powder. The individual powder grain size was assessed to be smaller than 50 µm in diameter. Initial experiments were performed with that pure oxide slag powder. However, as heterogeneous nucleation was observed during the melting procedure, it was decided to further homogenize the samples to prove if heterogeneous melting was causal for the observed crystallization.

Further homogenization was achieved by additional annealing of synthetic slag powder before it was used in the experiments. Ash fusion tests revealed an initial flow temperature of 1320 °C. However, to ensure fully oxide powder melting, the samples were annealed at 1550 °C for 5 h, resulting in a fully molten slag bulk. The annealing procedure was conducted in a high temperature furnace (HTF 18/8, Carbolite Gero GmbH & Co. KG, Neuhausen, Germany). Subsequently after the procedure, the annealed slag was crushed into particles with millimeter scale that were lastly used in the CLSM experiments.

CLSM Experiment

Confocal laser scanning microscopy (CLSM) provides an in situ view of a sample during heat treatment. Accordingly, the melting and solidification (crystallization) behavior can be determined with this setup. The high temperature furnace used in this study was manufactured by Lasertec (Model SVF17SP, Lasertec, Yokohama, Japan). The furnace chamber is comparably small (15–25 cm), oval-shaped (Fig. 1), and its inner surface is coated with gold (Fig. 2) [13, 14]. The chamber architecture and the coating are necessary for the furnace operation, since the heat is produced by a

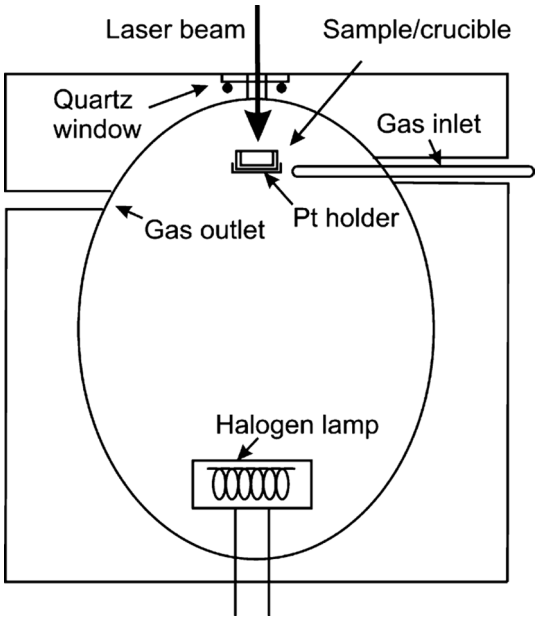

Fig. 1 Sketch of the high temperature furnace of the CLSM setup, as seen in [13] (Color figure online)

halogen lamp (Fig. 1). The lamp is operated by high voltage, to produce heat radiation. The radiation is reflected by the Au-coated inner furnace walls. Due to the oval shape, the heat radiation is focused in the upper region of the furnace, where the sample holder is located in the focus point of the heat radiation (Fig. 1) [13, 14]. Based on this architecture, high heating and cooling rates of approx. 300 K/min can be achieved in the used setup, due to the small furnace volume as well as no use of isolation material that could eventually store heat [13, 14]. On the sample holder, a sample containing crucible can be installed with dimension of a few millimeters (Fig. 2). Respectively, the sample amount is of limited extend. The sample holder incorporates a type-S thermocouple and the temperature calibration was conducted using the melting point of pure copper.

The furnace is sealed by a quartz glass window containing flange (Fig. 1). The sapphire glass window enables the observation of the sample by the confocal laser microscope that is located above the furnace unit. The microscope (Model 1LM21H, Lasertec, Yokohama, Japan) is equipped with several ocular lenses to adjust the magnification [14]. The CLSM is connected with a computer to display and store the images, as well as to operate the furnace heating. The experiments were performed using different atmospheres: Ar-gas and reduced Ar-gas. Ar-gas was used to display inert atmosphere with an oxygen partial pressure of $p(O_2) = 10^{-6}$ bar, due to contained oxygen impurities. Comparable partial pressures can be assumed in the early stages of slag formation in gasifiers [15]. However, the gasification atmosphere becomes reducing, as the fuel is converted into CO and H_2 by reacting with oxygen [15]. To apply such reducing conditions, a Mg-furnace was partly used to reduce the oxygen concentration in the Ar-gas (denominated as reduced Ar-gas) to different magnitudes, based on oxidation reactions of the Mg with the oxygen impurities. To examine the effect of oxygen partial pressure, experiments were conducted with inert Ar-gas and reduced Ar-gas atmosphere.

The experiments were performed using Pt- and Mo-crucibles. Pt was mainly used for inert atmosphere and Mo was used for the reduced atmosphere, due to intense oxidation behavior of Mo. The reducing atmosphere was assessed based on the oxidation state of the Mo-crucible. Its oxidation behavior was used as an oxygen partial pressure indicator. Some of the Mo-crucibles showed slight oxidation, some were fully reduced. Regarding the investigated temperatures (1100–1250 °C) and the partly oxidation of the crucibles, the present oxygen partial pressure with slight reducing

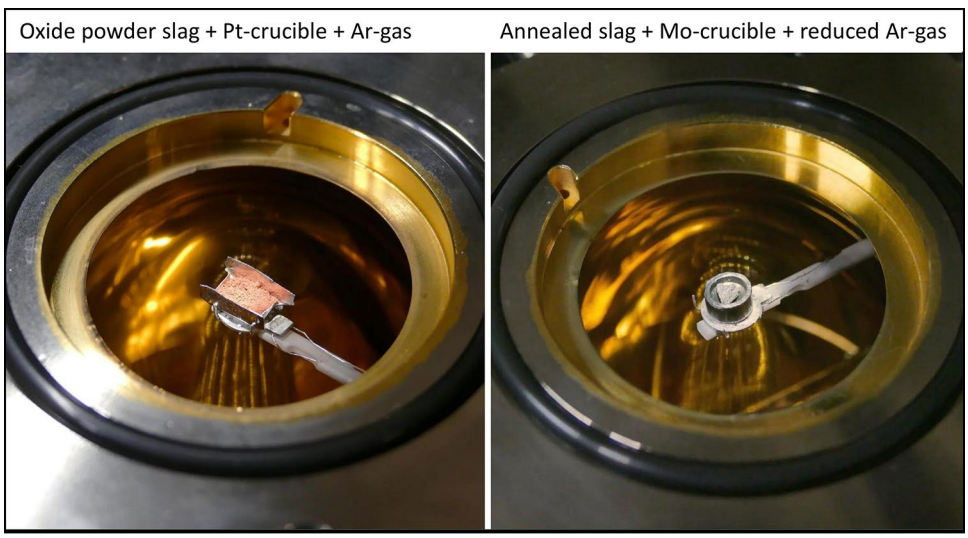

Fig. 2 The CLSM high temperature furnace, loaded with synthetic oxide powder in a Pt-crucible (left) and an annealed slag particle in a Mo-crucible (right) (Color figure online)

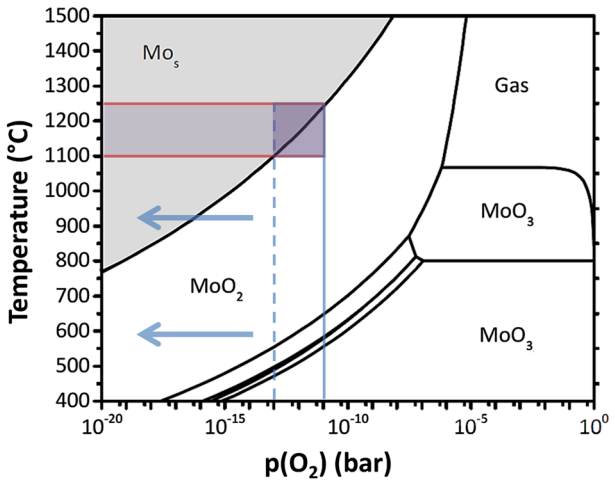

Fig. 3 Stability of the crucible material: molybdenum, calculated with FactSage and FactPS database. Figure modified after [12] (Color figure online)

atmosphere was assessed to be in average approx. 10^{-12} bar (including fluctuations between 10^{-11} and 10^{-13} bar) (Fig. 3). To monitor the magnitude of reducing conditions, the oxygen partial pressure was additionally monitored by an oxygen sensor (rapidox 2100, Cambridge Sensotec, St. Ives, Great Britain) and minimum oxygen partial pressures of up to 10^{-20} bar were detected during individual experiments.

As can be seen in Fig. 2, CLSM experiments were performed by varying the aforementioned parameters. Several experiments were performed with the combination of oxide powder in a Pt-crucible and Ar-gas ($p(O_2) = 10^{-6}$) to simulate the atmosphere in the early stage of conversion in a gasifier (Fig. 2). The atmosphere of the slag layer on the gasifier refractory walls was represented by experiments with slightly reduced Ar-gas ($p(O_2) = 10^{-12}$). As heterogeneous crystallization was observed due to the sample state of the oxide powder, annealed slag particles were used instead. The variations of oxygen partial pressure led to interactions of the Pt-crucibles with the slag, resulting in the choice of Mo-crucibles for further experiments (Fig. 2 right).

In the CLSM experiment, the samples were investigated isothermally. The main focus was set to the temperature range between 1100 and 1250 °C (Fig. 3). The samples were heated up with a rate of 50 K/min to observe the melting of the oxide powder, i.e., the annealed particle. The heating procedure was continued until a maximum temperature of 1500 °C was reached. To spare the setup components, it was decided to not reach higher temperatures. The samples were hold for 10 min at the maximum temperature and were subsequently cooled down to the target temperature of the investigation. Therefore, a high cooling rate of − 300 K/min was chosen. After the isothermal treatment, the samples were cooled to room temperature by also applying the cooling rate of − 300 K/min. Due to the high applied cooling rates, no influence of the cooling procedure on the crystallization phenomena was observed. However, a few experiments with a constant cooling rate of − 6 K/min were additionally performed to simulate slow cooling processes, as seen in Fig. 5. Additionally, a few experiments were performed under continuous cooling conditions, as seen in "Oxygen Partial Pressure" section.

Sample Analysis

The samples were investigated via optical microscopy for an initial analysis. Therefore, a KEYENCE VHX-S550E digital microscope (KEYENCE DEUTSCHLAND GmbH, Neu-Isenburg, Germany) was used. Crystallized regions of the sample were documented and crystallization structures could be determined. Microscopy can be used as a comparison with the CLSM images. Though, a maximum magnification of 200× was applied, higher resolution images were generated by SEM analysis. The analysis by SEM was conducted by Zeiss Merlin II and Supra 50 VP (Carl Zeiss Microscopy GmbH, Jena, Germany) devices. Furthermore, the analysis of the chemical composition of crystallized phases was performed by SEM–EDX analysis and element mappings.

Thermodynamic Equilibrium Calculations

Additionally, equilibrium calculations of the investigated slag systems were performed using Equilib program of the FactSage software package (version 7.2) in combination with GTox database (GTox is a private database) [16]. Calculation results were used as a reference to the experimental results. To examine the influence of the sample state, the crucible material, and the oxygen partial pressure, a comparison between both equilibrium calculations and experiments can give valuable information. Since the sample state and the crucible material cannot be regarded in the equilibrium calculations, two calculations were performed with different oxygen partial pressures. Firstly, a partial pressure of 10^{-6} bar was defined for the inert Ar-gas atmosphere. Secondly, the oxygen partial pressure of 10^{-12} bar was covered as a representative value for the reduced Ar-gas atmosphere.

Results

The influence of sample homogeneity, the crucible material, and the oxygen partial pressure on the crystallization of slag was investigated by CLSM experiments. The CLSM experiment can give insights on the above, since it provides in situ imaging of the investigated sample. Melting and solidification (crystallization) processes can be observed and are documented by digital imaging. Additionally, the

samples can be investigated after the experiment by optical microscopy and SEM analysis to gather further detailed insight on the sample behavior. Since the sample size is very limited, no additional XRD results could be performed. In this section, the influence of the sample state, the crucible material, and the applied atmosphere on the crystallization is displayed. The comparison of the crystallization phenomena, from samples applying different parameters, revealed that the quality of experimental results strongly depends on the assessed parameters. This study aims to contribute valuable information on the execution of CLSM experiments that can be used to improve future experimental studies.

Equilibrium Calculations

Firstly, equilibrium calculations were performed to predict the crystallization products of the investigated synthetic HKR slag system (Fig. 4). Since the sample state and the influence of the crucible material cannot be represented by such calculations, the oxygen partial pressure was changed as a variable. Factsage Equilib calculations were conducted for oxygen partial pressures of 10^{-6} and 10^{-12} bar, representing inert Ar-gas and reduced Ar-gas atmospheres (Fig. 4), as explained in "CLSM Experiment" section.

According to the calculations, the liquidus and the solidus temperature display only minor deviations, based on the diverging atmosphere (Fig. 4). For the reduced Ar-gas, two slag phases were predicted, based on the reduction of the Fe_2O_3 to FeO species. The crystallizing phases are spinel, olivine, melilite, anorthite ($CaAl_2Si_2O_8$), and clinopyroxene. Due to the variations of the oxygen partial pressure, the fraction of the crystallized phases varies. At reduced atmosphere, the content of crystallized olivine increased at lower temperatures, while the content of melilite and spinel decreased and fluctuated, respectively (Fig. 4). Anorthite is present at low temperatures of approx. 1130 °C for both atmospheres. Clinopyroxene was calculated for inert atmosphere, but not for the reduced conditions. The variations of the crystallized phase fractions are explained by the reduction of Fe_2O_3 species by the reducing atmosphere, since the Fe_2O_3 species is very sensitive to the oxygen partial pressure [17].

State of Sample

The influence of the sample state was documented in experiments using synthetic oxide powder slag in Pt-crucibles at inert Ar-gas atmosphere. To display the influence of the sample state, an isothermally investigated (1159 °C) sample was chosen. As can be seen in Fig. 5a, the slag powder melts heterogeneously during heating. In consideration of the individual melting points of oxidic compounds, this behavior is reasonable. In the following, at peak temperatures of 1500 °C, the liquid slag droplets showed inner crystallized structures (Fig. 5b). The CLSM image indicates the presence of some crystals with a maximum diameter of approximately 20 mm. By comparing this image with Fig. 5c, the same particles can still be identified in the slag. However, their polygonal morphologies are visible more clearly. Image 5c was captured during cooling at 1175 °C, indicating that the particles have grown ever since the peak temperature between. The SEM–EDS image 5d displays the morphology in more detail. BSE-EDX analysis revealed a Mg–Fe–Al composition. Regarding the Equilib calculations, the polygonal shape, and the silica-free composition, the phase was identified as a spinel with a high likelihood. It can be concluded that the spinel crystals grew due to heterogeneous

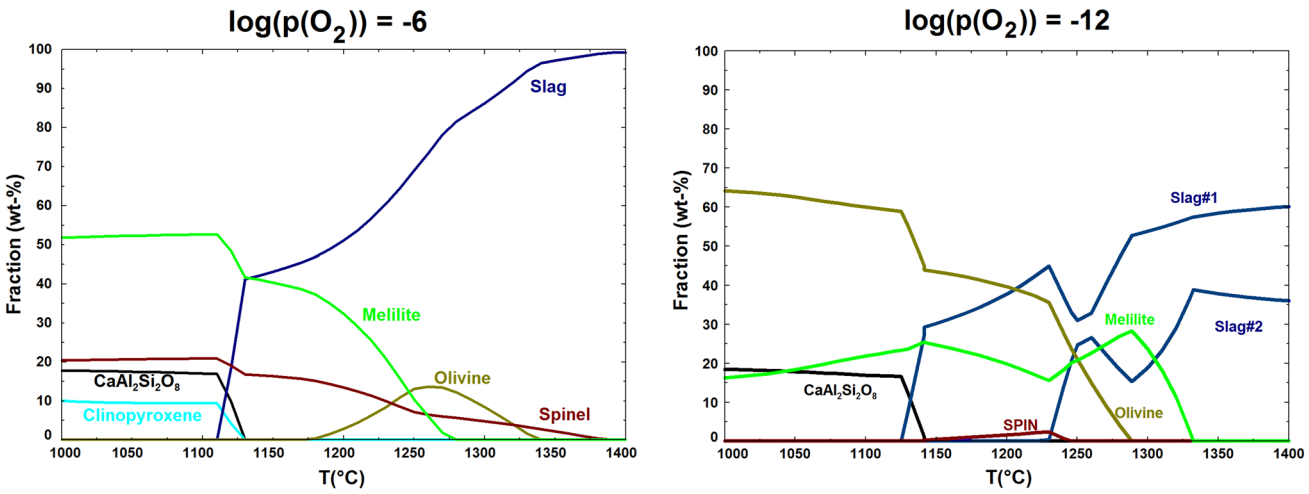

Fig. 4 FactSage Equilib calculations for the synthetic HKR slag system, performed for different oxygen partial pressures, representing inert Ar-gas (left) and reduced Ar-gas (right) (Color figure online)

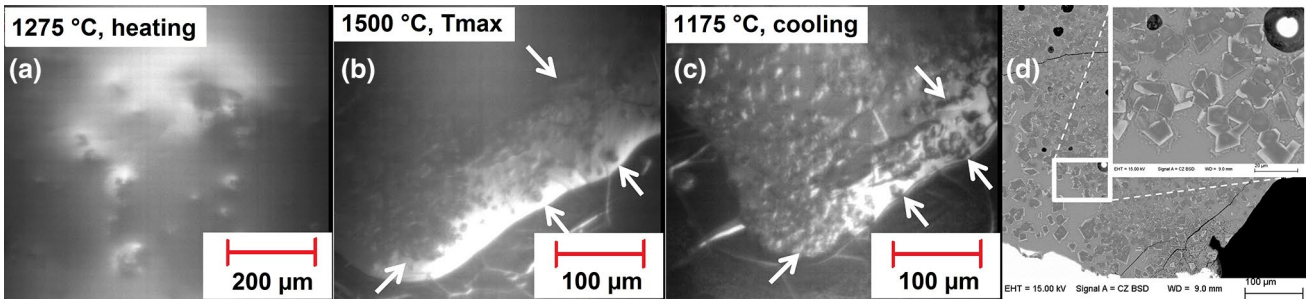

Fig. 5 Synthetic HKR slag powder on Pt-crucible at Ar-gas atmosphere. **a** Heterogeneous melting at 1260 °C. **b** crystals in the slag at $T_{max} = 1500$ °C. **c** Crystals at 1160 °C. **d** SEM–EDS image of crystalline phase (Color figure online)

nucleation during the heating procedure. On the one hand, partial melting of oxides leads to locally different slag compositions and additionally, the remaining oxide particles in the liquid slag can be used as a nucleus for the crystals to grow. Nonetheless, the crystallization was triggered by the heterogeneous melting, the presence of the spinel phase displays accordance with the results of the equilibrium calculations, and no foreign phases were identified. However, since the investigation of crystallization processes in gasifier slags requires comparable homogeneous nucleation, a homogeneous liquid slag bulk must be ensured to produce reliable data.

The same sample was further investigated. As indicated by Fig. 6, the ascertained spinel crystals were present in small slag droplets on the Pt-crucible. However, larger slag droplets are found at the corners of the crucible and the crystallization products have different shapes. As this area was investigated via SEM–EDS, other phases were likely identified, based on their composition and the predictions by equilibrium calculations (Fig. 6). Large crystals with olivine composition formed in the slag. Their shapes are dendritic and they are accompanied by a zone of heterogeneous crystallization. In such zones, crystals with melilite and clinopyroxene composition grew besides each other in one-dimensional and dendritic shape, respectively. Also very small polygonal crystals of spinel composition have been found. With increasing distance to the large olivine crystals, the slag displays a fine-grained crystallized area (Fig. 6), which composition could not be identified, due to the small grain size.

Regarding the ascertained spinels shown in Fig. 5 and the crystallization zone (Fig. 6) of the slag droplet in the crucible edge, the crystallization zones are barely comparable with each other. Nonetheless, the documented phases represent only barely accordance with the predicted phases from the equilibrium calculations (Fig. 4). At the investigated temperature of 1150 °C, only melilite and spinel crystals are supposed to grow. The crystallization of olivine (only above 1180 °C) and clinopyroxene (only below 1130 °C) are the major deviations from the equilibrium calculations. Due to the heterogeneous growth of spinels, however, the chemical composition of the bulk slag changed. Accordingly, this is causal for the deviation of the crystallized phases from the initially performed calculations. Furthermore, it can be seen that the large slag droplet showed also signs of polygonal spinel crystals on the droplet margin (Fig. 6). Regarding

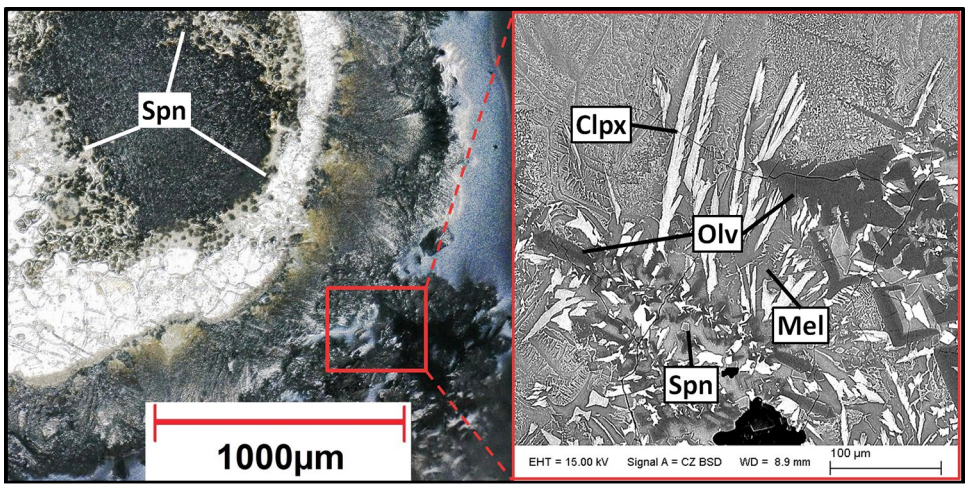

Fig. 6 Microscopic image (left) and SEM–BSE image (right) of the same sample shown in Fig. 5. The small droplet is seen in the top-left and the large droplet in the bottom and right region (left). The composition of the phases were analyzed via SEM–EDS. Based on the composition and regarding equilibrium calculations they were identified as *Clpx* clinopyroxene, *Olv* olivine, *Mel* melilite, *Spn* spinel (Color figure online)

the lack of such spinels on the top of large droplet (Fig. 6), it can be argued that the heterogeneous nucleation could be supported as the slag is in contact with the Pt-crucible. However, due to the crucible design and its limited dimensions, no vertical cross section could be prepared to validate the crystallization change with respect to the Pt-crucible distance.

Oxygen Partial Pressure

CLSM investigations also exposed an impact on the crystallization characteristics with respect to the applied oxygen partial pressure. Firstly, an Ar-gas atmosphere was set for the experiments. Regarding oxygen impurities, an O_2 partial pressure of about 10^{-6} bar was applied during the experiment (Fig. 7). The results were compared with another experiment, adding an Mg-furnace to reduce the oxygen concentration in the Ar-gas atmosphere. To exclude any influence from the crucible material, the experiments were performed, using Mo-crucible for both experiments. For the Ar-gas atmosphere, the Mo-crucible formed an oxide layer, due to the comparable high oxygen partial pressure (Fig. 3). Furthermore, annealed slag particles were used in these experiments instead of slag oxide powder to exclude the influence of heterogeneous nucleation, as concluded in the previous chapter. The samples displayed in Fig. 7 were constantly cooled with − 6 K/min to compare the temperatures of initial crystallization and to compare crystal growth.

The distinctions in the crystallization tendency of the two different reducing regimes were major. As displayed in Fig. 7a, distinct small crystals were firstly observed at temperatures of 1380 °C under Ar-gas. Under reduced Ar-gas, however, no crystallization could be observed at this temperature. Figure 7b was chosen, as it marks the temperature of the first crystallization in the experiment using reduced Ar-gas. The displayed, pyramidal crystal grew to a size of approx. 170 µm in diameter within 54 s, resulting in a growth rate of 3 µm/s. In contrast, the sample under Ar-gas showed proceeding crystallization of smaller polygonal crystals in which individual crystal size barely increased. Figure 7c represents the temperatures of total solidification, i.e., crystallization at 988 °C and 993 °C, respectively.

On the one hand, the sample with reduced Ar-gas experienced a higher individual crystal growth rate, but lower initial crystallization temperature. On the other hand, the sample treated with regular Ar-gas displayed contrary behavior. The solidus temperature of both experiments indicates a strong kinetic shift to lower temperatures (approx. 990 °C), since the solidus temperature was predicted at approx. 1120 °C (Figs. 4, 7). The higher crystal growth rate of the experiment using reduced Ar-gas can be explained by the transformation of Fe_2O_3 to FeO, due to the low oxygen partial pressure. Fe_2O_3 is defined as an amphoter that can potentially increase the viscosity of the slag [18]. An increase in the slag viscosity is associated with lower diffusion and therefore lower atom mobility. Contrarily, FeO is a network modifier that disrupts silicate structures in the slag, decreases the viscosity, and improves the atom mobility [18]. Hence, crystal growth processes are supposed to be faster. It must be noted that a further reduction of the Fe_2O_3 species can be neglected, since pure iron was not identified in the samples.

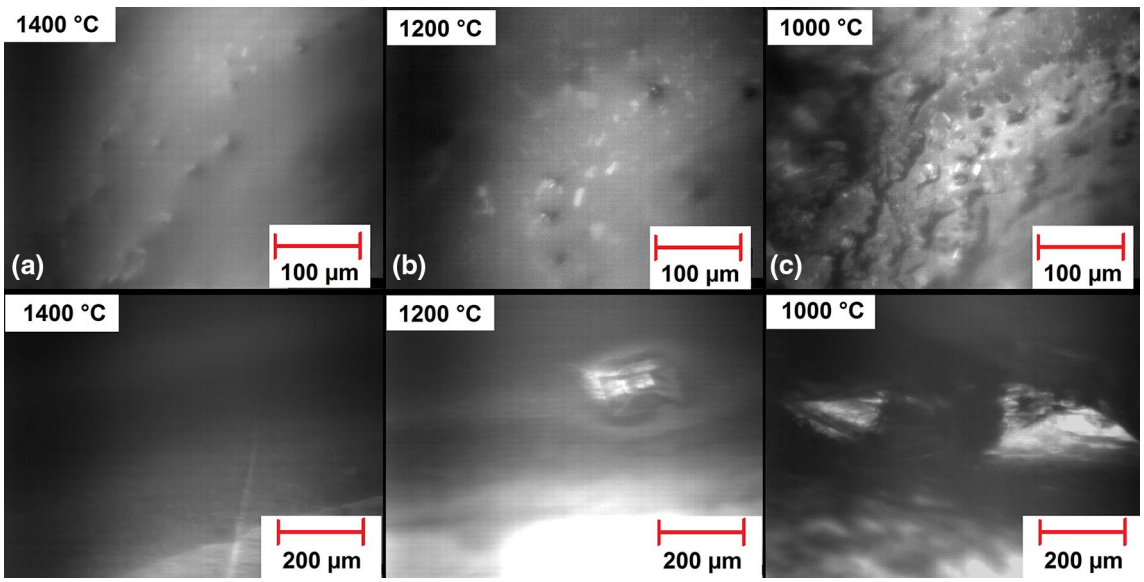

Fig. 7 Comparison of two experimental runs containing pre-annealed HKR slag in Mo-crucibles. **a** 1380 °C, **b** 1160/1153 °C, **c** 988/993 °C (Color figure online)

Crucible Material

The crucible material is a significant factor when it comes to experimental studies. Common crucible materials are platinum, corundum, and molybdenum. Corundum (Al_2O_3) is an impropriate material for oxidic slag systems as it can be dissolved in the slag itself. In contrast, platinum is commonly used for these systems due to its general chemical inertness and its high melting point. Molybdenum, instead, is hard to process and tends to oxidize, though its high melting point is an advantage. To prove possible influence of the crucible material, CLSM experiments were performed in Pt-crucibles, followed by Mo-crucibles. To also neglect the influence of heterogeneous nucleation, annealed slag particles were used. By flushing the furnace with Ar-atmosphere, no certain interaction was documented between the Pt-crucible and the synthetic HKR slag.

However, as the Ar-atmosphere was reduced by using the Mg-furnace subsequently, HKR slag behaved differently. As slag droplets flowed over the Pt-crucible bottom during the heating procedure and at the peak temperature, the laser beam was reflected poorly on these areas. Accordingly, the Pt-crucible experienced an alteration due to the interaction with the slag. Furthermore, slag droplets suddenly disappeared from the Pt-crucible, by flowing into cracks and wholes of the crucible bottom. Since the crucible was intact before the experiment, all cracks and wholes formed during the experiment. Figure 8 displays frayed holes in the crucible bottom that occurred during the experiment, based on the mentioned interaction with slag.

These frayed structures indicate an involvement of chemical processes and excludes the probability of a material failure due to bending and folding. This finding can be explained by the reduction of Fe_2O_3 to FeO and lastly to pure Fe. Fe subsequently formed a Pt–Fe-alloy with the crucible. Consequently, the melting point of the alloy is lower than the peak temperature of 1500 °C, so the alloy liquefied and the integrity of the crucible failed. Further experiments with Mo-crucibles and comparable atmosphere have been performed. Though, for the same applied experimental conditions, the formation of completely reduced Fe was never observed. Due to its catalytic properties, Pt enhanced the reduction of Fe_2O_3 in the slag and formed the Fe–Pt-alloy already after a few minutes of exposure. In contrast, Mo has no such catalytic influence, so that Fe_2O_3 was not reduced to pure Fe. However, the formation of FeO species, as mentioned in other studies [17], seems reasonable, due to the higher crystal growth rate that is caused by lower viscosities of the slag [18] ("Oxygen Partial Pressure" section). Though, the tendency of Pt to form alloys with other metals is known, the fact that certain areas of the Pt-crucible bottom (Fig. 8b, estimated 1000 μm^2) with a crucible thickness of 100 µm got completely dissolved is meaningful. Regarding the fact that the underlying sample holder incorporates a type-S thermocouple that is made up of a Pt–Rh-alloy, such crucible failure can lead to significant damage of the CLSM sample holder and shall be prevented. In Fig. 8b, the underlying Al_2O_3 powder is visible through the crucible whole. After finishing this experimental run, the crucible was attached to some of the Al_2O_3 powder, which bound the released slag. If CLSM experiments with comparable parameters are conducted, a thin layer of Al_2O_3 powder between the crucible and the sample holder can be used to take up the released slag, as applied in this study (Fig. 8b). Furthermore, to completely neglect the risk of a crucible failure and the formation of an Pt–Fe-alloy, Mo-crucibles are recommended for the analysis of oxidic slag systems in the CLSM setup. Nonetheless, it must be noted that a certain degree of reduced atmosphere is required for Mo-crucibles, otherwise the crucible experiences oxidation (Fig. 3).

Comparison of Crystallization Products

Since sufficient evidence has been provided for the impact of each of the experimental parameters, the influence on the crystallization characteristics is discussed in this section. The results displayed in this section are representative for samples investigated under the experimental parameters described in Fig. 2: oxide slag powder + Pt-crucible + Ar-gas

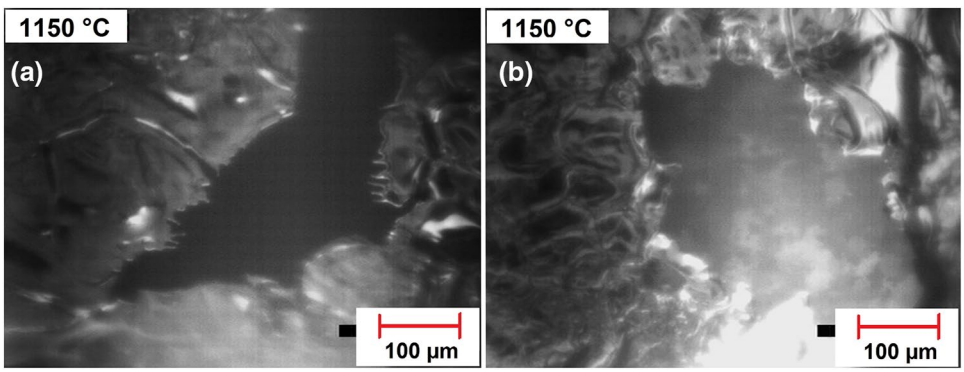

Fig. 8 Damaged Pt-crucible due to Pt–Fe-alloy forming, observed in the CLSM (Color figure online)

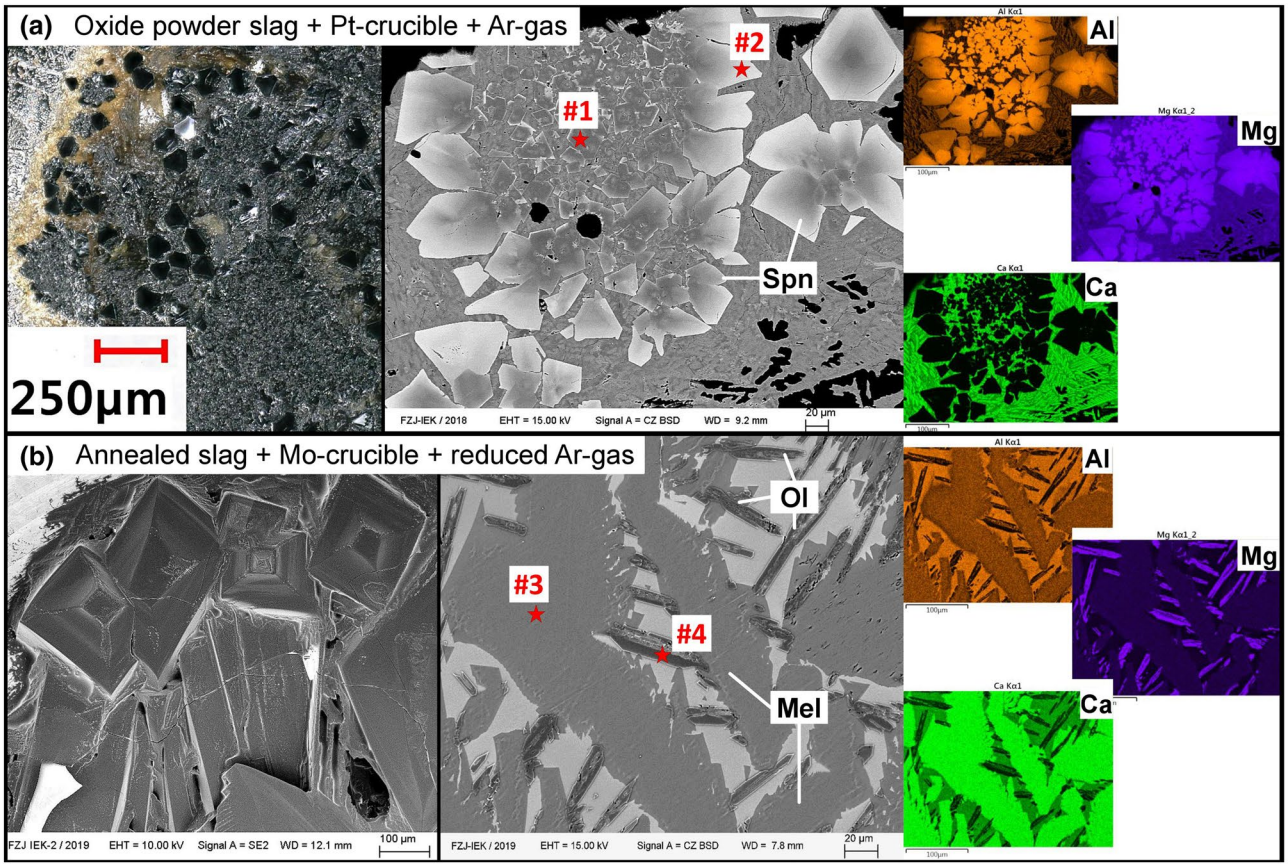

Fig. 9 Comparison of two analyzed samples in the CLSM setup. **a** HKR powder sample in a Pt-crucible under inert Ar-gas and **b** annealed HKR slag particle in a Mo-crucible under reduced Ar-gas. The left images show the sample surface by an optical microscopic (**a**) and a SEM (**b**) image. The middle column shows SEM–BSE images with SEM–EDX point measurements of the sample cross section. On the right side, Al (orange), Mg (purple), Ca (green) SEM–EDX mappings of the same cross section are shown (Color figure online)

and annealed slag particle + Mo-crucible + reduced Ar-gas (Fig. 9). Additional comparison was made with previous crystallization results of synthetic HKR slag, investigated in a quenching experiment with identical parameters [19].

As shown in Fig. 5, synthetic HKR slag powder led to heterogeneous nucleation during the heating procedure. Figure 5d further displayed the presence of distinct polygonal crystals that were ascertained as spinel in the small slag droplet. The same phase was documented in a constantly cooled (− 75 K/min) CLSM sample, as shown in Fig. 9a. The sample surface also contained very planar polygonal and relatively large crystals, as documented by microscopic imaging (Fig. 9a). SEM–BSE image of a sample cross section (Fig. 9a) also revealed the dominance of that polygonal phase. The selected SEM–EDX elemental mappings indicate enrichment in Fe and Mg, but a very strong depletion and no fraction of Ca (Fig. 9a) and Si (Table 2), respectively.

The SEM–EDX point measurements (Table 2) additionally prove the content of Mg, Al, Fe, and O. Furthermore, the comparison of #1 and #2 indicates that the composition of that phase varies: the inner region is enriched in Al and the outer region is depleted in Al, but enriched in Fe (Table 2). Regarding the contrast of the

Table 2 Composition of the SEM–EDX point measurements in at.%, as displayed in Fig. 9

	O	Mg	Al	Si	Ca	Fe
#1	54.7	13.7	22.5	0.0	0.1	9.2
#2	54.9	13.5	14.5	0.0	0.1	17.0
#3	57.5	5.5	4.8	14.8	16.8	0.6
#4	55.9	22.6	0.3	14.4	1.8	5.0

SEM–BSE images, these composition changes are crystal zone formations and indicate a miscibility of several elements having diverging atom masses. Regarding the predicted phases by FactSage equilibrium calculations and the chemical composition, the polygonal phase of Fig. 9a was identified as spinel with great certainty. The surrounding slag showed traces of dendritic crystals, but a characteristic chemical composition for any other crystallized phase could not be determined, due to the small crystal size.

The sample shown in Fig. 9b, however, consisted of a slag particle that was annealed and investigated in a Mo-crucible under reduced Ar-gas atmosphere. SEM–BSE image of the sample surface showed symmetric square to rectangular pyramidal crystals (Fig. 9b) that have a similar morphology compared to the crystals already displayed in Fig. 7b, c, indicating that they belong to the same crystal phase. Such shaped crystals have also been determined in the previous study and were identified as melilite. Crystals with the aforementioned spinel morphology were only present as very small crystals with subordinate fractions (not displayed). Regarding the SEM–EDX point measurements (Fig. 9b, Table 2), the large skeletal phase consists of Ca, Si, Al, and Mg. By taking further SEM–EDX point measurements into account, the skeletal phase shows slight fluctuations of the Mg, Al, and Si contents in behalf of each other. In contrast, the Ca fractions remained constant. The composition correlates well with a miscibility crystal of gehlenite (1/3) and åkermanite (2/3) of the melilite group. Including the Equilib results (Fig. 4), and recent findings [19], the large skeletal phase was identified as the melilite phase (Fig. 9b, #3). Contrary, the second elongated phase displays a different composition (Fig. 9b #4, Table 2). The fraction of Mg is highly enriched, while Ca is strongly depleted and Al is almost not incorporated in the crystal (Table 2, #4). Incorporating its composition and the predicted phases via equilibrium calculations, the phase was identified as olivine. The presence of an olivine phase is also in very well agreement with quenching results of synthetic HKR slag in previous studies [19]. Due to the chemical composition, it is a miscibility crystal made up by fayalite, forsterite, and monticellite. The element mappings clearly display the enrichment of Mg in olivine and the enrichment of Ca in melilite. As described above, previous study of the analyzed synthetic HKR slag system in a quenching experiment has proven the growth of melilite and olivine [19]. The accordance of the morphology and chemical composition of the crystallized phases in this work with previous study clearly confirm the repeatability of the experimental results [19]. On the other hand, the crystallization products for slag powder in Pt-crucibles and inert Ar-gas atmosphere (Figs. 5, 6, 9a) display only a vague accordance. In addition to the deviations to the equilibrium calculations for inert Ar-gas, a clear influence of the diverging parameters on the slag crystallization was determined.

Conclusion

An experimental study on the crystallization characteristics of oxidic slag systems was conducted by using the CLSM setup [3]. To validate the impact of the sample state, the applied oxygen partial pressure, and the crucible material, several experiments were performed. For each of these parameters, different effects on the slag crystallization were documented. A comparison with the parameters synthetic fine-grained slag powder, Pt-crucibles, and inter Ar-gas was made with the following: annealed slag particles (1550 °C, 5 h holding time), Mo-crucibles, and reduced Ar-gas. The effect of parameter substitution was determined as follows:

- State of sample: heating of oxide slag powder led to heterogeneous melting, resulting in local fluctuations of the bulk slag chemistry. Accordingly, crystalline phases grew heterogeneously in the partial liquid slag. Once the crystals formed, the slag bulk chemistry has changed and the subsequent crystallization is not representative, as also indicated by deviations towards FactSage Equilib calculation results. It was recommended to anneal the slag samples before the experiment at temperatures appropriately above the liquidus temperature. The use of annealed slag particles creates a homogeneous slag bulk, eliminating the probability of heterogeneous nucleation.
- Impact of oxygen partial pressure: due to the grade of reducing atmosphere, different crystallization behaviors were observed. Higher O_2 partial pressures led to high-temperature-shifted crystallization with low growth velocities, while reduced Ar-gas allowed higher grades of supercooling and, therefore, high crystallization kinetics. It was argued that the O_2-sensitive Fe_2O_3 species was responsible for the observed behavior. Oxygen partial pressure of 10^{-12} bar reduced Fe_2O_3 to FeO species which is categorized as a network modifier. The FeO species resulted in lower slag viscosity and higher atom mobility that lastly enabled a high degree of supercooling and larger crystal growth rates.
- Influence of crucible material: it was documented that Pt-crucibles in combination with Fe-containing slags form a Pt–Fe-alloy under reducing conditions, also due to the reduction of Fe_2O_3. This alloy has a low melting point and is responsible for crucible failure. It was advised against the use of Pt-crucibles for Fe-rich slags at reduc-

ing conditions. To ensure the integrity of the experimental setup and the reproducibility of results, the crucible material Mo was suggested, as it is not forming alloys and has high temperature stability. However, low oxygen partial pressure is required to prevent Mo oxidation.

For Fe-containing oxidic slag systems, the consideration of the abovementioned advices led to crystallization products that display improved accordance with FactSage equilibrium calculations. Additionally, crystallization investigations in a quenching experiment with annealed synthetic HKR slag, Mo-crucibles, and reducing atmosphere [19] are also in very well agreement with the CLSM results shown in this study. It can be concluded that experimental parameters: sample state, crucible material, and partial pressure of oxygen influence the crystallization processes. The fact that annealed slag, Mo-crucibles, and reduced atmosphere generate comparable results between two different experiments, clearly state that the experimental setup itself has no impact on the comparability of results.

Acknowledgements Open Access funding provided by Projekt DEAL. This work was supported by the Federal Ministry for Economic Affairs and Energy on the basis of a decision by the German Bundestag within the project "HotVeGas" (FKZ 0327773 K).

Compliance with Ethical Standards

Conflict of interest The authors declare no competing financial interest.

References

1. Seebold S et al (2017) The influence of crystallization on the flow of coal ash-slags. Fuel 187:376–387
2. Wu GX et al (2015) Viscosity model for oxide melts relevant to fuel slags. Part 2: the system SiO_2-Al_2O_3-CaO-MgO-Na_2O-K_2O. Fuel Process Technol 138:520–553
3. Schwitalla DH et al (2017) Analysis of solid phase formation and its impact on slag rheology. Fuel 203:932–941
4. Johne PK et al (2018) Fuel & load-flexible entrained flow gasifier operation & applications: flame parameters & flexible burner. 27th International Conference on the Impact of Fuel Quality on Power Production and the Environment, Lake Louise, Canada
5. DeYoung S (2018) CFD simulations of an industrial scale entrained flow gasifier: Influence of gasifier design and operating conditions. 9th International Freiberg Conference on IGCC & XtL Technologies, Berlin, Germany
6. Xuan W et al (2017) Influence of silica and alumina ($SiO_2 + Al_2O_3$) on crystallization characteristics of synthetic coal slags. Fuel 189:39–45
7. Liu Z et al (2018) Effect of crystallization on the abrupt viscosity increase during the slag cooling process. ISIJ Int 58(11):1972–1978
8. Xuan W et al (2015) Influence of SiO2/Al2O3 on crystallization characteristics of synthetic coal slags. Fuel 144:103–110
9. Xuan W et al (2014) Influence of CaO on crystallization characteristics of synthetic coal slags. Energy Fuels 28(10):6627–6634
10. Esfahani S, Barati M (2016) Effect of slag composition on the crystallization of synthetic CaO–SiO2–Al2O3–MgO slags: part I- Crystallization behavior. J Non-Cryst Solids 436:35–43
11. Park J, Ryu J, Sohn I (2014) In-situ crystallization of highly volatile commercial mold flux using an isolated observation system in the confocal laser scanning microscope. Metall Mater Trans B 45(4):1186–1191
12. Seebold S (2017) Über den Einfluss der Kristallisation auf das Fließverhalten oxidischer Schmelzen, Dissertation, Fakultät für Maschinenwesen. 2017, Rheinisch-Westfälische Technische Hochschule Aachen: Aachen. p 168
13. Jones PT et al (2007) Using confocal scanning laser microscopy for the in situ study of high-temperature behaviour of complex ceramic materials. J Eur Ceram Soc 27(12):3497–3507
14. Liu Z et al (2017) Effect of crystallization on the abrupt viscosity increase during the slag cooling process. ISIJ Int 58(11):1972–1978
15. Spliethoff H (2010) Power generation from solid fuels. Springer-Verlag, Berlin Heidelberg, p 647
16. Hack K, Jantzen T, Müller M, Yazhenskikh E, Wu G (2012) A novel thermodynamic database for slag systems and refractory materials. Proceedings of the 5th International Congress on the Science and Technology of Steelmaking. Dresden, Germany
17. Xuan W et al (2015) Influence of Fe_2O_3 and atmosphere on crystallization characteristics of synthetic coal slags. Energy Fuels 29(1):405–412
18. Vargas S et al (2001) Rheological properties of high-temperature melts of coal ashes and other silicates. Prog Energy Combust Sci 27(3):237–429
19. Schupsky JP et al (2019) Investigations on crystallisation processes of three oxidic gasifier slag systems. Proceedings of the 44th International Technical Conference on Clean Energy. Clearwater, Florida, pp 253–265